Polypyridyl ruthenium complexes containing anchoring nitrile groups as TiO$_2$ sensitizers for application in solar cells

Juan H. Mecchia Ortiz [a], Claudia Longo [b,*], Néstor E. Katz [a,*]

[a] INQUINOA-CONICET, Instituto de Química Física, Facultad de Bioquímica, Química y Farmacia, Universidad Nacional de Tucumán, Ayacucho 471, (T4000INI) S. M. de Tucumán, Argentina
[b] Institute of Chemistry, University of Campinas, UNICAMP, C. Postal 6154, 13083-970 Campinas, SP, Brazil

A B S T R A C T

Ruthenium polypyridyl complexes of general formula [Ru(bpy)$_{3-x}$(Mebpy-CN)$_x$]$^{2+}$ (x = 1,2 and 3, bpy = 2,2'-bipyridine, Mebpy-CN = 4-methyl-2,2'-bipyridine-4'-carbonitrile) can be used as visible dyes in novel solar cells formed with a porous TiO$_2$ film (1 cm^2), Pt counter-electrode and iodine/iodide as the redox mediator electrolyte dissolved in a polymeric matrix. These complexes can be anchored over the surface of nanocrystalline TiO$_2$ through nitrile groups, as evidenced by Raman spectra of the adsorbed species. Irradiated by a solar simulator (67 mW cm^{-2}), the cells assembled with the Ru complexes with x = 2 and 3 as TiO$_2$ sensitizers exhibit almost identical current–potential curves, with short-circuit photocurrents of 1.25 mA cm^{-2}, fill factors of 0.5 and overall efficiencies around 0.44%. The Ru complex with x = 1 and a similar Re complex did not perform as well as sensitizers. These data were consistent with results obtained from quantum efficiency curves and impedance spectra. We conclude that complexes with nitrile groups as anchoring entities are promising candidates for designing efficient DSCCs.

© 2015 Elsevier B.V. All rights reserved.

The replacement of fossil fuels by renewable energy sources is a big challenge to scientists [1]. Grätzel's type dye-sensitized TiO$_2$ solar cells (DSSC) can be considered a promising technology for solar energy conversion in the near future [2]. Many different photosensitizers have been tested, such as transition metal complexes [3], organic dyes [4] and, more recently, perovskites [5].

It is well known that the majority of sensitizers are bonded to the semiconductor surface through carboxylic acid groups [6]. Different binding modes of these groups are possible, such as ester linkage, chelate binding, bidentate bridges and so on. Other anchoring groups have also been described, such as phosphonic acid, boronic acid, silanes and other moieties [6]. We have recently reported the possibility of using nitrile groups as anchoring entities over ZnO nanowires [7]. One of the advantages of having nitriles as binding groups is that no agglomeration is possible in ZnO surfaces, thus opening the way to having more robust and efficient materials for use as sensitizers in DSSCs. However, no reports on the usage of ruthenium photosensitizers containing nitrile substituents as anchoring groups over TiO$_2$ in a prototype of a DSSC have been published up to date.

Therefore, we address in this work the feasibility of new DSSCs having ruthenium species anchored to the surface of TiO$_2$ particles by nitrile groups. We have selected for this research the previously described complexes of formulae: [Ru(bpy)$_2$(Mebpy-CN)]$^{2+}$ (RuL1),

[Ru(bpy)(Mebpy-CN)$_2$]$^{2+}$ (RuL2), [Ru(Mebpy-CN)$_3$]$^{2+}$ (RuL3), and [Re(Mebpy-CN)(CO)$_3$Cl] (ReL) (bpy = 2,2'-bipyridine, Mebpy-CN = 4-methyl-2,2'-bipyridine-4'-carbonitrile) [7,8], whose structures are shown in Supplementary Scheme 1. The efficiency of DSSCs sensitized with these complexes have been determined and compared to the standard dye N719 (Ruthenizer 535-bis TBA from Solaronix).

First, sensitized TiO$_2$ mesoporous films were prepared and characterized. The TiO$_2$ films were deposited by the doctor blade technique, from an aqueous suspension containing nanocrystalline TiO$_2$ particles (diameter ca. 25 nm, from HPW Catalysts & Chemicals Ind. Co., Ltd.) and Renex® onto transparent electrodes, glass covered with a conductive film of F-doped SnO$_2$ (glass-FTO, 15 Ω/sq, TCO22-15 Solaronix S.A.), followed by thermal treatment (30 min at 350 °C and 30 min at 450 °C). This procedure guarantees the gradual and complete removal of organic components, resulting in a uniform film of interconnected TiO$_2$ particles, ca. 1.5 μm thick [9]. The TiO$_2$ electrodes were dipped into 1 × 10^{-3} mol L^{-1} acetonitrile solutions of ReL and the PF$_6^-$ salts of RuL1, RuL2, and RuL3 and maintained for 10–12 h; the electrodes were afterwards rinsed with acetonitrile. The stability of nitrile group binding over the semiconductor's surface for all complexes was checked by immersion of the sensitized film in 3 mL of acetonitrile and acetone for 1 week. No desorbed complexes were detected by UV–Visible spectroscopy neither in acetone nor in acetonitrile. The normalized UV–Visible spectra of the complexes adsorbed over TiO$_2$ films are displayed in Supplementary Fig. S1; they are very similar to UV–Visible spectra previously measured in acetonitrile solutions, with RuL1, RuL2 and RuL3 absorbing at λ$_{max}$ = 454, 473 and 471 nm, respectively [7].

* Corresponding authors.
E-mail addresses: clalongo@iqm.unicamp.br (C. Longo), nkatz@fbqf.unt.edu.ar (N.E. Katz).

Fig. 1 shows the comparative Raman spectra recorded for each sensitizer (as a pure solid) and for the sensitized TiO_2 film (Raman DXR spectrometer from Thermo Scientific equipped with a binocular Olympus Microscope). The nitrile stretching frequency appearing at 2240 cm^{-1} in the pure PF_6^- salts of complexes RuL1, RuL2 and RuL3 is displaced to 2333 cm^{-1} in the same complexes adsorbed onto TiO_2. This positive shift of $\Delta\nu = 93$ cm^{-1} is a clear indication of chemical adsorption and can be attributed to coordination of the free N of the nitrile group to a Ti^{4+} center. A frequency shift of $\Delta\nu = 50$–70 cm^{-1} has been previously detected for nitrile-coordinated complexes of transition metals in high oxidation states [10]. Moreover, the displacement is much higher than that observed when these complexes are adsorbed onto ZnO [7], as expected because TiO_2 exhibits higher charge of the semiconductor metal center than ZnO. In $(RuL1)(PF_6)_2$ and $(RuL2)(PF_6)_2$ no bands at 2240 cm^{-1} are detected, but in $(RuL3)(PF_6)_2$ both bands (at 2333 and 2234 cm^{-1}) are observed, pointing to the fact that in this last species two nitriles bind to the surface while the third nitrile group remains free. In ReL, the frequency shift is similar to that recorded for Ru complexes ($\Delta\nu = 81$ cm^{-1}).

The quantity of sensitizer adsorbed on the TiO_2 films (Γ_{ad}) is an important parameter for the DSSC performance. This parameter was determined for each complex after immersing a sensitized film in a 1 mol L^{-1} aqueous KOH solution for 4 h. This procedure promotes a complete desorption due to the hydrolysis of the nitrile group and its substitution by the OH^- group. The UV–Visible spectra of the solutions were measured afterwards and the complex concentrations were estimated considering the sensitizer absorption extinction coefficients [7,8,11]. The Γ_{ad} values (Table 1) can be associated to the number of nitriles in the complex structure. Thus, Ru1 and ReL, with only one nitrile group per molecule, exhibited almost the same value of Γ_{ad} (0.03 μmol cm^{-2}), while the 30% higher values observed for RuL2 and RuL3 (*ca.* 0.04 μmol cm^{-2}),

Table 1
Quantity of complex adsorbed on the semiconductor surface and energy levels of the states involved in dye-sensitized TiO_2 electrodes.

Dye	Γ_{ad}/μmol/cm^2	$E_{1/2}$/V[a]	E_{0-0}/eV	$E_{1/2}$*/V
RuL1	0.030	1.23	1.98	−0.75
RuL2	0.042	1.32	1.87	−0.55
RuL3	0.040	1.36	1.90	−0.54
ReL	0.029	1.33	2.16	−0.83

[a] *vs.* NHE, 0.1 M TBAHP in acetonitrile.

can be probably attributed to the two potentially anchoring nitrile groups. These Γ_{ad} values are similar to those determined for other Ru dyes adsorbed onto TiO_2 surfaces [12]. Table 1 also shows additional physicochemical properties of the four sensitizers adsorbed onto TiO_2. The oxidative potentials for the metallic centers ($E_{1/2}$) of the adsorbed species were measured by cyclic voltammetry in acetonitrile solutions with tetra-n-butylammonium hexafluorophosphate (TBAHP) and are very similar to those measured for the complexes dissolved in acetonitrile [7,8]. These potentials are higher than the redox potential of the I^-/I_3^- couple (~0.4 eV *vs.* NHE) thus supplying a favorable thermodynamic driving force for dye regeneration. The energy difference between the first excited state and the ground state (E_{0-0}) were determined by a single mode fit of the steady-state emission spectra already reported [7,8]. The oxidative potentials for the metallic centers in the first excited states ($E_{1/2}$*) were determined by the difference: $E_{1/2}^* = E_{1/2} - E_{0-0}$. These values must be higher than the equilibrium Fermi level on the semiconductor for obtaining a moderate exoergonicity for the charge injection process [13]. The values of $E_{1/2}^*$ for RuL2 and RuL3 are very close to the value of the equilibrium Fermi level on TiO_2 mesoporous film with adsorbed N719 (−0.5 eV) [13]. The higher
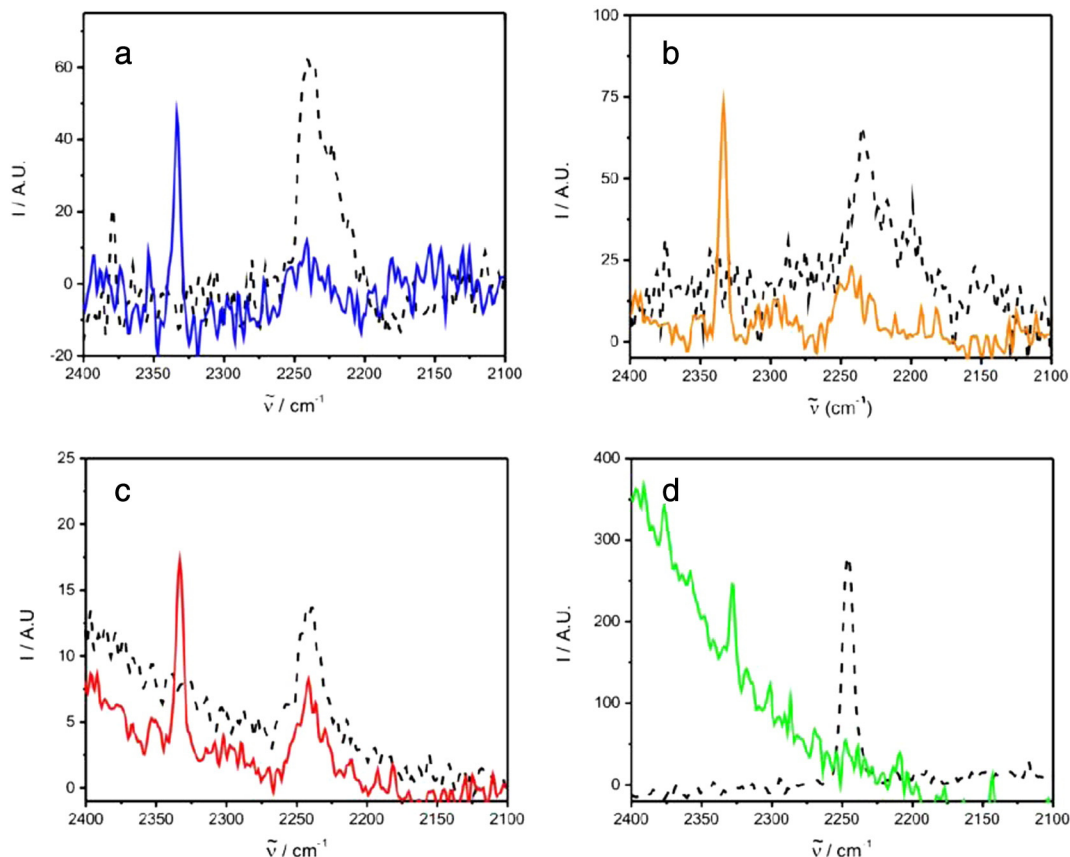

Fig. 1. Raman spectra recorded for pure solids (dashed lines) and for TiO_2 mesoporous films sensitized from acetonitrile solutions (full lines) of (a): $(RuL1)(PF_6)_2$; (b): $(RuL2)(PF_6)_2$; (c): $(RuL3)(PF_6)_2$ and (d): ReL.

charge of the complexes described in this work decreases the Fermi Level to *ca.* -0.2 eV.

Considering the stability and favorable properties obtained for the sensitized TiO_2 electrodes, they were also used for assembling DSSCs with a polymer electrolyte. First, the Pt-layered glass-FTO used as counter-electrodes were freshly prepared by coating a solution 0.05 mol L^{-1} of H_2PtCl_6 in isopropanol followed by heating at 380 °C for 30 min. The polymer electrolyte consisted of the redox couple I_3^-/I^- dissolved in a polymer matrix of poly(ethylene oxide), PEO, and poly(vinylidene-fluoride-co-hexafluoro-propylene), PEO/PVdF-HFP. Initially, a solution was prepared by dissolving NaI (75 mg), I_2 (8 mg), PVdF-HFP (50 mg) and PEO (500 mg) in acetone (40 mL) and acetonitrile (10 mL), under magnetic stirring. Then, a film of the polymer electrolyte was deposited on the surface of freshly prepared sensitized TiO_2 electrodes (1 cm^2) by casting (12 aliquots of 1 mL) at 40 °C, using adhesive tape as spacers (40 μm). Once the solvent was almost completely evaporated resulting in a semifluid gel, the counter-electrode was placed in a sandwich configuration; crocodile tweezers were used to uniformly press both electrodes until the polymer electrolyte film was completely dried. Using this procedure, the ionic conductivity for this polymer electrolyte corresponded to 0.3 mS cm^{-1} [14]. For comparison, a similar solar cell was also assembled using the complex N719 (Solaronix S.A.), of formula $[Ru(L)_2(SCN)_2](TBA)_2$ (L = 4,4′-dicarboxy-2,2′-bipyridine).

The performance of each DSSC for solar energy conversion was evaluated using the Quantum Efficiency/Incident Photon to Charge Carrier Efficiency (QE/IPCE) Newport measurement kit (consisting of a 300 W ozone free Xe lamp, chopper, monochromator, detector and other accessories). Also, the cells were irradiated using a "homemade" solar simulator and current–potential curves and electrochemical impedance spectroscopy (EIS) measurements were registered using a potentiostat/galvanostat (Ecochemie Autolab PGSTAT 128-N), with a Frequency Response Analyser (FRA) module. The solar simulator was assembled with a metallic vapor lamp (Metalarc Sylvania HIS-YHX 400 W) and, considering the distance from the lamp and solar cell, 25 cm, the polychromatic irradiance was estimated as 67 ± 5 mW cm^{-2}.

The QE spectra of the solar cells, acquired under ambient temperature (25 ± 1 °C), are represented in Fig. 2a. Fig. 2b shows the current–potential curves obtained under irradiation with the solar simulator (linear sweep voltammetry, 5 mV s^{-1}) at 30 ± 1 °C.

In Fig. 2a, except for the solar cell assembled with ReL sensitized TiO_2, the higher efficiencies were observed for incident radiation with wavelength ranging from 460 to 520 nm, in excellent correspondence with the UV–visible spectra of sensitized TiO_2 films (Fig. S1). Comparison of QE and I–V curves revealed that the cells assembled using RuL2 or RuL3 as TiO_2 sensitizers showed a very similar performance under irradiation, exhibiting almost identical short-circuit photocurrents ($I_{SC} = 1.25$ mA cm^{-2}), maximum power and overall efficiency values ($P_{max} = 0.3$ mW cm^{-2}, $\eta = 0.44\%$), as displayed in Table 2. Moreover, in spite of the fact that RuL2 and RuL3 solar cells exhibited different QE profiles, the areas under these curves are almost identical. On the other hand, for the RuL1 sensitized TiO_2 solar cell, a 36% smaller area is obtained from the QE curve; also, the I_{SC}, P_{max} and η values are ca. 36% smaller than those exhibited for RuL2 and RuL3 solar cells, suggesting that for these RuL sensitizers, the cell performance for light conversion can be associated with the amount of adsorbed complex on TiO_2 (Γ_{ad} values, Table 1). However, since Γ_{ad} values were similar for ReL and RuL1, the poorest performance exhibited by the ReL solar cell cannot be related to the ReL adsorption on the TiO_2 film, but to its very low absorption in the visible region.

These results revealed that all the Ru complexes described in this work exhibited a reasonable yield of energy conversion compared with the extensively studied complex N719, since in the same conditions the N719 sensitized TiO_2 solar cell exhibited $I_{SC} = 1.42$ mA cm^{-2}, $V_{oc} = 0.70$ V, $P_{max} = 0.47$ mW cm^{-2}, $ff = 0.47$ and $\eta = 0.70\%$ (Supplementary Fig. S2). The lower V_{oc} exhibited by the cells assembled with these Ru
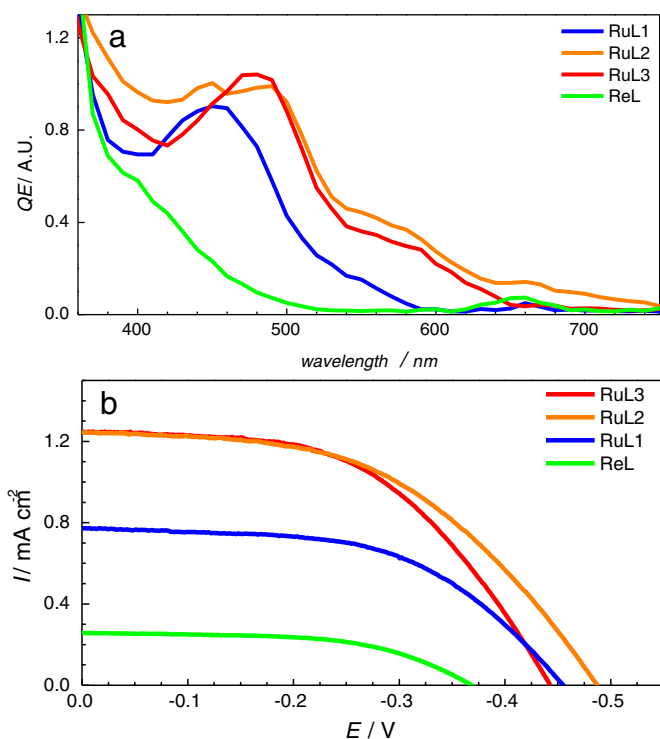

Fig. 2. Solar cells (1 cm^2) assembled with the sensitized TiO_2, Pt counter-electrode and a polymer electrolyte: (a) quantum efficiencies spectra and (b) current–potential curves under polychromatic irradiation.

complexes, compared to that observed for a similar N719 cell can be attributed to the 2 + positive charge of the ruthenium centers. It is well known that the conduction band edge of a mesoporous TiO_2 film depends on the charge on the surface of the semiconductor [15,16]. V_{oc} depends also on the quantity of complexes chemisorbed over the surface. The much lower value of V_{oc} for the Re complex is related to a lower degree of electron injection due to its lowest absorption in the visible region [17].

Supplementary Fig. S3 presents the Impedance spectra obtained for irradiated solar cells, using a perturbation of ± 10 mV over the open circuit potential, in a frequency range from 5 mHz to 50 kHz. The EIS results were analyzed using Boukamp software; therefore, in Fig. S3, symbols correspond to the experimental data while solid lines represent the fit obtained using the equivalent circuit $R_S [C_1 (R_1O_1)] (R_2Q_2)$, as previously discussed [9]. In this circuit, R and C describe resistances and capacitances respectively; O, associated with the parameters Y_{o1} and B, can represent a finite-length Warburg diffusion (Z_{Dif}) in a finite-length region of length l_e (which might be the thickness between the electrodes, 40 μm), and Q is the symbol for the constant phase element, CPE (associated with the $Y_{o,2}$ and n parameters) [9].

As shown in Table 3, the impedance at high frequency, associated to the ohmic resistance of R_S element, ranged from 40 to 52 Ω for these devices and can be mainly attributed to the polymer electrolyte resistance. The sub-circuit $[C_1 (R_1O_1)]$ can represent the capacitance and charge-transfer resistance at the Pt|electrolyte interface (frequencies from 0.1 to 1 kHz), also accounting for the diffusion of electroactive species in

Table 2
Parameters obtained from I–V curves for the dye-sensitized TiO_2 solar cells under polychromatic irradiation ((67 ± 5) mW cm^{-2}).

Dye	V_{oc}/V	I_{sc}/mA cm^{-2}	P_{theo}/mW cm^{-2}	P_{max}/mW cm^{-2}	ff	$\%\eta$
RuL1	0.45	0.77	0.35	0.19	0.54	0.28
RuL2	0.49	1.25	0.61	0.30	0.49	0.45
RuL3	0.44	1.25	0.55	0.29	0.53	0.43
ReL	0.37	0.26	0.096	0.053	0.55	0.079

$P_{theo} = V_{oc} I_{sc}$; $P_{max} = I_{max}V_{max}$; $ff = (P_{max}/P_{theo})$; η = overall efficiency.

Table 3
Parameters obtained by fitting the impedance spectra of irradiated dye-sensitized TiO_2 solar cells (1 cm^2) using the R_S [C_1 (R_1O)] (R_2Q) equivalent circuit (shown as an inset in Figure S3a).

Dye	$\chi^2 \times 10^4$	R_S/Ω	$C_1/\mu F$	R_1/Ω	Y_{o1}/S	$B/s^{1/2}$	R_2/Ω	$Y_{o2}/mF\ s^{n-1}$	n
RuL1	2.9	51	44	15	0.068	2.4	96	1.18	0.86
RuL2	1.5	42	23	16	0.142	3.0	53	0.97	0.69
RuL3	1.5	52	30	17	0.104	2.3	53	0.95	0.74
ReL	3.3	41	268	16	0.043	3.5	278	0.43	0.93

the polymer electrolyte (low frequency response). Except for the ReL–TiO_2 solar cell, R_1 corresponded to (16 ± 1) Ω and C_1 ranged from 23 to 44 μF for these devices. The resistance diffusion (R_{Dif}), which is associated to the B/Y_{o1} ratio, corresponded to 22 Ω for RuL2 and RuL3 solar cells; higher values were estimated for devices assembled using RuL1 and ReL as sensitizers, 35 and 81 Ω, respectively. Finally, considering the parameters of the sub-circuit (R_2Q_2), which can be associated with the medium-frequency response for the TiO_2|electrolyte interface, similar values were obtained for the RuL2 and RuL3 sensitized TiO_2 solar cells while higher resistances were obtained for the RuL and ReL devices. The fitting was very good, as shown by the values of χ^2.

Comparison of Nyquist diagrams (Fig. S3a) and the parameters presented in Table 3 revealed that cells with RuL2 and RuL3 exhibit the lowest impedance values, in consistency with their QE and I–V curves. Finally, the cell with ReL, with the highest impedance values, is also the least efficient.

The values of the fill factors ff and the efficiencies η shown in Table 2 are similar to those determined for Ru complexes adsorbed onto TiO_2 modified with cyclodextrins [12]. It is noteworthy that for the RuL2 and RuL3 complexes, these values are close to those for N719, because of their higher number of anchoring groups. We conclude that ruthenium bipyridyls substituted with nitrile groups are promising candidates for designing efficient DSSCs.

Acknowledgments

Appendix A. Supplementary material

Structures of complexes, UV–Vis spectra of dye-sensitized TiO_2 electrodes, current–potential curve for a solar cell assembled with N-719-sensitized TiO_2 electrode and impedance spectra for the irradiated solar cells. Supplementary data to this article can be found online at http://dx.doi.org/10.1016/j.inoche.2015.03.009.

References

[1] R. Eisenberg, D. Nocera, Inorg. Chem. 44 (2005) 6799.
[2] M. Grätzel, Acc. Chem. Res. 42 (2009) 1788.
[3] J.-F. Yin, M. Velayudham, D. Bhattacharya, H.-C. Lin, K.-L. Lu, Coord. Chem. Rev. 256 (2012) 3008.
[4] F. Castellano, J. Photochem. Photobiol. A Chem. 223 (2011) 57.
[5] N.K. Noel, S.D. Stranks, A. Abate, C. Wehrenfennig, S. Guarnera, A.-A. Haghighirad, A. Sadhanala, G.E. Eperon, S.K. Pathak, M.B. Johnston, A. Petrozza, L.M. Herzaand, H.J. Snaith, Energy Environ. Sci. 7 (2014) 3061.
[6] A. Reynal, E. Palomares, Eur. J. Inorg. Chem. (2011) 4509.
[7] J.H. Mecchia Ortiz, N. Vega, D. Comedi, M. Tirado, I. Romero, X. Fontrodona, T. Parella, F.E. Morán Vieyra, C.D. Borsarelli, N.E. Katz, Inorg. Chem. 52 (2013) 4950.
[8] J.H. Mecchia Ortiz, F.E. Morán Vieyra, C.D. Borsarelli, I. Romero, X. Fontrodona, T. Parella, N.D. Lis de Katz, F. Fagalde, N.E. Katz, Eur. J. Inorg. Chem. (2014) 3359.
[9] C. Longo, A.F. Nogueira, M.A. Paoli, H. Cachet, J. Phys. Chem. B 106 (2002) 1925.
[10] R.D. Foust Jr., P.C. Ford, Inorg. Chem. 11 (1972) 899.
[11] The complete desorption of the complex was checked by measuring the UV–Visible spectra of the films, re-immersing the films in KOH solutions and then immersing in ethanol-acetonitrile (1:1) mixtures. No bands corresponding to the sensitizers were detected on the films.
[12] J.A. Bonacin, S.H. Toma, J.N. Freitas, A.F. Nogueira, H.E. Toma, Inorg. Chem. Commun. 36 (2013) 35.
[13] C.A. Bignozzi, R. Argazzi, R. Boaretto, E. Busatto, S. Carli, F. Ronconi, S. Caramori, Coord. Chem. Rev. 257 (2013) 1472.
[14] B.H. Oliveira, Msc. Thesis, Unicamp, 2011.
[15] M.K. Nazeeruddin, R. Humphry-Baker, P. Liska, M. Grätzel, J. Phys. Chem. B 107 (2003) 8981.
[16] K. Fredin, J. Nissfolk, G. Boschloo, A. Hagfeldt, J. Electroanal. Chem. 609 (2007) 55.
[17] F. Labat, T. Le Bahers, I. Ciofini, C. Adamo, Acc. Chem. Res. 45 (2012) 1268.